IEEE Photonics Journal
An IEEE Photonics Society Publication

Open Access

On Laser Ranging Based on High-Speed/Energy Laser Diode Pulses and Single-Photon Detection Techniques

Volume 7, Number 2, April 2015

Juha Kostamovaara, Senior Member, IEEE
Jaakko Huikari
Lauri Hallman
Ilkka Nissinen, Member, IEEE
Jan Nissinen
Harri Rapakko
Eugene Avrutin, Member, IEEE
Boris Ryvkin

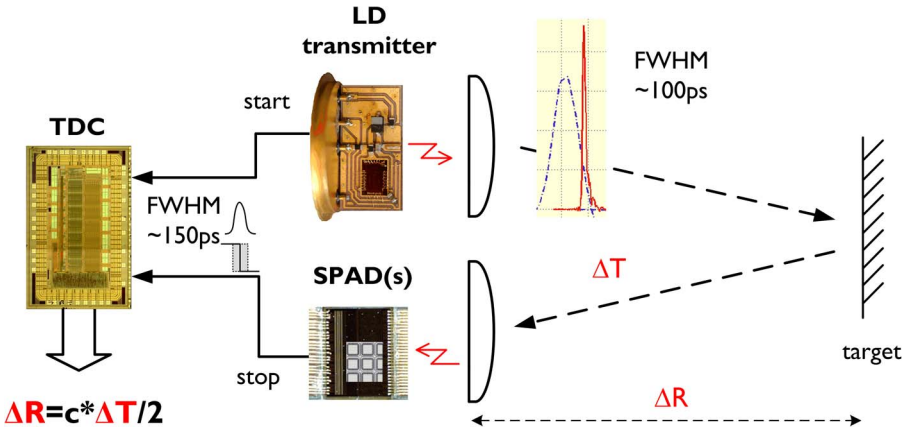

DOI: 10.1109/JPHOT.2015.2402129
1943-0655

On Laser Ranging Based on High-Speed/Energy Laser Diode Pulses and Single-Photon Detection Techniques

Juha Kostamovaara,[1] *Senior Member, IEEE*, Jaakko Huikari,[1] Lauri Hallman,[1] Ilkka Nissinen,[1] *Member, IEEE*, Jan Nissinen,[1] Harri Rapakko,[1] Eugene Avrutin,[2] *Member, IEEE*, and Boris Ryvkin[1,3]

[1]Electronics Laboratory, Department of Electrical Engineering, University of Oulu, 90014 Oulu, Finland
[2]Department of Electronics, University of York, York YO10 5DD, U.K.
[3]A. F. Ioffe Physico-Technical Institute, 194021 St. Petersburg, Russia

DOI: 10.1109/JPHOT.2015.2402129

Manuscript received December 10, 2014; revised February 4, 2015; accepted February 4, 2015. Date of current version February 25, 2015. This work was supported in part by the Academy of Finland through the Centre of Excellence in Laser Scanning Research under Contract 272196, Contract 255359, Contract 263705, and Contract 251571, and in part by TEKES. Corresponding author: J. Kostamovaara (e-mail: juha.kostamovaara@ee.oulu.fi).

Abstract: This paper discusses the construction principles and performance of a pulsed time-of-flight (TOF) laser radar based on high-speed (FWHM ∼100 ps) and high-energy (∼1 nJ) optical transmitter pulses produced with a specific laser diode working in an "enhanced gain-switching" regime and based on single-photon detection in the receiver. It is shown by analysis and experiments that single-shot precision at the level of 2…3 cm is achievable. The effective measurement rate can exceed 10 kHz to a noncooperative target (20% reflectivity) at a distance of > 50 m, with an effective receiver aperture size of 2.5 cm^2. The effect of background illumination is analyzed. It is shown that the gating of the SPAD detector is an effective means to avoid the blocking of the receiver in a high-level background illumination case. A brief comparison with pulsed TOF laser radars employing linear detection techniques is also made.

Index Terms: Instrumentation, sensors, laser radar, pulsed time-of-flight, single photon detection.

1. Introduction

Optical time-of-flight (TOF) radars are typically based on either continuous wave (CW) phase comparison method or on measurement of the transit time of a short laser pulse to the target and back to the receiver [1]. These techniques are advantageous compared to microwave radars, for example, since they have good spatial accuracy and also have potential for low-cost. The spatial accuracy arises from the fact that at optical frequencies the transmitted beam can easily be collimated with optical lenses. Thus, the accuracy is good not only in the direction of the optical axis but also in the transversal direction. It has been shown that both the CW and pulsed TOF methods can give high accuracy at a millimeter level within a wide measurement range. They have found applications in proximity sensors in the measurement of level heights in silos and containers, in positioning of tools and vehicles, and in the measurement of geometrical size and shape of objects, for example [2], [3].

There has been, however, a growing interest in applying these techniques in areas beyond the traditional applications mentioned above. It is foreseen that the measurement of 3-D data will be quite essential for many control and navigation applications. Development of an autonomous, or "driverless" car, is one example of such an activity that obviously calls for high-speed environment-sensing techniques [4], [5]. In these applications, the pulsed time-of-flight technique is typically preferred due to its high measurement speed and capability to deal with multiple echoes, for example. Moreover, it is also widely accepted that low-cost 3-D imaging in particular would have great potential for opening up a wide field of applications in surveying, map capturing, consumer electronics (games), robotics (man-machine interfaces), medical techniques, and the controlling of machines (gesture control), for example [6].

Traditionally, linear detection methods based typically on an avalanche photo diode (APD) detector have been used in pulsed-time-of-flight laser radars [3]. This kind of radar requires thus a sensitive analog receiver that amplifies the current signal from the APD to a suitable voltage level for further signal processing. It is also well known that in optical pulse-mode radars, unlike in microwave radars, at a constant energy level a shorter pulse gives not only improved time resolution but also a better signal-to noise ratio (SNR) [7]. A pulsed TOF laser radar aiming at a distance range of tens of meters to non-cooperative targets calls typically for a pulse power of 20..30 W with reasonable dimensions of optics. This pulse power level can be achieved from pulsed laser diodes with a peak current of $>$ 20 A typically. The laser driver is usually based on utilizing the avalanche breakdown in a bipolar junction transistor or on a MOS switch. In these drivers the minimum width of the current pulse (and thus of the laser pulse) is typically limited to 3–5 ns [8]–[10].

In addition to the linear detection mode, recently, there has been increasing interest in using single photon detection techniques (SPAD) in connection with laser radars. Both phase [11]–[13] and pulse modulated transmitter configurations have been used [14]–[16]. It appears however that at least for the long range applications ($> 20-30$ m) with non-cooperative targets the most promising results have so far been achieved with the pulsed time-of-flight direct detection architecture. In the recent study, Niclass *et al.* used a laser pulse with a peak power and length of 40 W and 4 ns, respectively, and a SPAD based receiver to construct a laser scanner for a traffic application [16]. While the results are promising and encouraging as such, it is obvious that the long laser pulse used poses a trade-off with regard to the precision achievable and complexity of the signal processing needed for the required accuracy. This trade-off arises because in the simplest form of the single photon detection there is no a priori knowledge on the position of the detected photon within the pulse envelope. Thus, a pulse width of 5 ns would give an inherent uncertainty of 1 meter in distance measurement in the single photon detection mode. Better precision can be achieved but only at the cost of using more photons (higher SNR or longer measurement time) for the detection. An obvious improvement would then be the shortening of the laser diode output pulse but, as already mentioned, the readily available driver techniques do not allow this at the required current and power level.

Another possibility of decreasing the laser diode output pulse width is to utilize the natural relaxation oscillations of the laser cavity. In the gain-switching mode, a laser diode can indeed produce a short (30–100 ps at half maximum) optical pulse when pumped with current pulses of nanosecond durations [17]. Unfortunately, however, in order to realize the true gain switching regime, with a single output pulse free from significant trail of secondary pulses, the amplitude of the pumping current pulse cannot exceed a certain value. This, in turn, limits the peak power of the optical pulse, the typical maximum value being of the order of a few hundred milliwatts or less with "standard" off-the-shelf laser designs. It should also be noted that the highest current pulse amplitude that gives a single optical pulse, and hence the power and energy of this optical pulse, can be increased somewhat by decreasing the pumping pulse duration. However, utilizing this route with "standard" laser diodes tends to require an ultra-high speed driver $(t_r < \sim 200$ ps$)$ making miniaturization of the transmitter at the required power level impossible. This requirement arises from the known fact that for fully realizing the potential of gain-switching the rise time of the driver current pulse should be less than the inherent lasing delay of the laser diode. Thus,

the power level available from a gain switched laser diode would seriously limit the measurement range and/or measurement time in the single photon detection mode [15].

In our recent work, we have however proposed a new laser diode structure which can inherently, and while placing much less strict speed requirements on the driver, produce high energy ($>$ 1 nJ) and high-speed optical pulses (pulse width $\sim$100 ps) with a high pulsing rate [18]–[22]. The main idea is to use a structure with a large "equivalent spot size" $(d_{act}/\Gamma > 2.5\ \mu m)$, with d_{act} and Γ being the active layer thickness and confinement coefficient, respectively. Such a laser design is somewhat unusual (for lasers with wide, $>$ 5 μm, stripe width), since the increase in d_{act}/Γ radically increases the lasing threshold current. From the point of view of dynamic behavior, however, the use of this special design results, as we have shown, in "enhanced gain-switching" and eventually in an efficient picosecond operation mode [18], [22]. In the case of bulk or Quantum Well (QW) edge-emitting lasers, the large equivalent spot size can in principle be achieved in markedly asymmetric waveguide structures, which also have the advantage of supporting only a single fundamental transverse mode for any stripe width. By comparison with alternative high-power transmitter designs based on master oscillator optical power amplifiers or photonic band crystal laser diodes [23], [24], this has the advantage of a much simpler construction as well as promising better pulse performance. Moreover, the principle referred to above $(d_{act}/\Gamma \gg)$ is a general one, implying that it works with all types of laser diodes. The notable fact is that the width of this high energy laser pulse matches with the typical single shot timing precision of a SPAD, which is 50–100 ps, and, thus, ensures a single shot precision of the order of 150 ps $(<$ 3 cm$)$ in pulsed time-of-light laser radar. Thus the limitation on precision set by the pulse length of the order of several nanoseconds disappears.

The hypothesis set forth in this paper is that with the laser diode introduced above and utilizing "enhanced gain switching" and with single photon detection techniques realized in standard CMOS technology, it is possible to construct very compact pulsed time-of-flight laser radars and imagers (2-D, 3-D) with high performance in terms of precision and measurement range. In fact, the proposed laser radar concept can be considered a fully digital laser radar sensor, since it uses "impulses" as its probe signals and "digital detection" in the receiver.

In what follows, we will first give, in Section 2, a more detailed description of the proposed laser radar architecture and its components. In Section 3, we briefly analyze the performance with respect to the available signal-to-noise ratio. One of the key issues in single photon detection is the effect of background radiation induced triggerings, which will be discussed in Section 3 as well. In Section 4, we will describe the measurement configuration and Section 5 will present the measurement results from a prototype realization confirming the conclusions made. Finally, conclusions and a summary of the study are given in Section 6.

2. Construction of the SPAD Based Laser Radar

2.1. System Configuration

The pulsed time-of-flight (TOF) laser distance measurement method is based on the measurement of the transit time (ΔT) of a short laser pulse to an optically visible target and back to the receiver. Since the velocity of light is known with high accuracy, the distance to the target can be calculated from

$$R = c \cdot \frac{\Delta T}{2}. \tag{1}$$

A block diagram of a pulsed time-of-flight laser radar is shown in Fig. 1. In the proposed architecture the transmitter consists of a laser diode working in the enhanced gain switching mode, and its driver, both of which are described in more detail below. The receiver consists of a single photon detector or a detector array depending on the measurement configuration and application aimed at. A SPAD detector is in fact a reverse biased diode which is biased above its breakdown voltage. In that case, any instance of an electron-hole pair generation (as a result

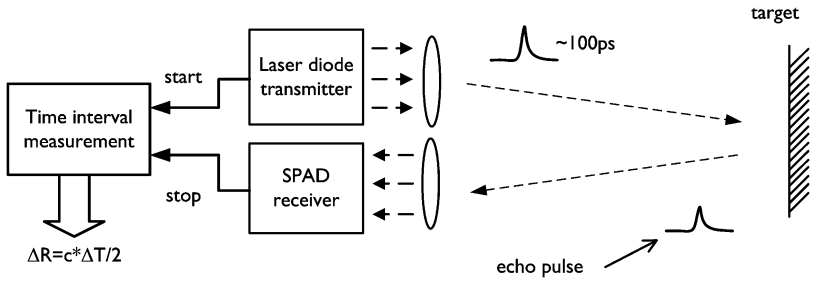

Fig. 1. Block diagram of a pulsed TOF laser range-finder.

of photon absorption, for example) within the depleted region of the junction may induce avalanche breakdown, resulting in a "digital-like" output signal [25]. SPAD detectors or detector arrays can be realized in standard CMOS technologies of varying area and configuration. They have low timing jitter, of the order of 50 ps, and a photon detection probability typically of 2–35% (wavelength dependent) and require no analog signal processing, unlike devices such as linear APDs. Moreover, they allow high circuit and system integration levels, since the detector chip can include other necessary electronics as well.

The third main block is the time interval measurement unit (time-to-digital converter, TDC) calculating the time difference between the start and stop pulses. It is shown elsewhere, see for example [26] and references therein, that a TDC can be realized as a multi-channel integrated circuit achieving a single shot precision of 10 ps (sigma value) within a measurement range of 100 μs, for example. Thus a high performance TDC and a SPAD detector or a detector array can both be manufactured on a single CMOS die as is already shown in earlier studies [16], [27]. Thus, from the point-of-view of system integration, the critical element is the laser diode transmitter, which will be discussed next.

2.2. Laser Diode Transmitter

We have shown earlier that the enhanced gain switching principle can be applied to any kind of a laser diode. In particular, we have demonstrated its use theoretically and experimentally with bulk and quantum well (QW) edge emitting laser diodes and, theoretically, with Vertical Cavity Surface Emitting Lasers (VCSELs) [21], [22], [28]. In the experiments described below, we have used a bulk double heterostructure (DH) laser diode grown in the GaAs/GaAlAs material system and operating at the wavelength of $\sim$870 nm. The laser diode used had a stripe width and cavity length of 30 μm and 3 mm, respectively. The divergence of the far-field pattern is approximately 13° (fast axis, half maximum light power angle). At the wavelength of 870 nm, the typical Si SPAD photon detection probability is of the order of 2–3% [29]. With a QW laser design in the same material system, the wavelength can easily be reduced to around 800 nm, which would enhance the photon detection probability to about 5% [29].

The critical system level parameters of the laser diode transmitter are its output pulse properties (energy level, pulse width), pulsing rate and overall complexity. The optical output pulse shape (red curve) and the corresponding pulse current (blue curve) measured from above the bulk laser diode transmitter are shown in Fig. 2. Note that these results are separate measurements at different current levels, combined in one figure for easy comparison. With a peak current amplitude of $\sim$6.5 A, for example, the laser diode gives a peak power of $\sim$9 W and pulse width (FWHM)of 125 ps. Thus, the pulse energy is $\sim$1 nJ.

The laser diode driver was realized with a MOS switch and an LCR transient-based pulse shape control. The principle of the driving scheme and the actual circuit board used are shown in Fig. 3 and would, without the extra connectors needed for testing, occupy a circuit board area of 1–2 cm^2. Since the current pulses driven through the laser diode are quite short ($\sim$1 ns, which is achievable with a MOS driver up to 10 A, see [30]), the average current at a pulsing rate of, say, 100 kHz, is only 0.5 mA. Thus a high pulsing rate of 100 kHz–1 MHz can be achieved, which is a

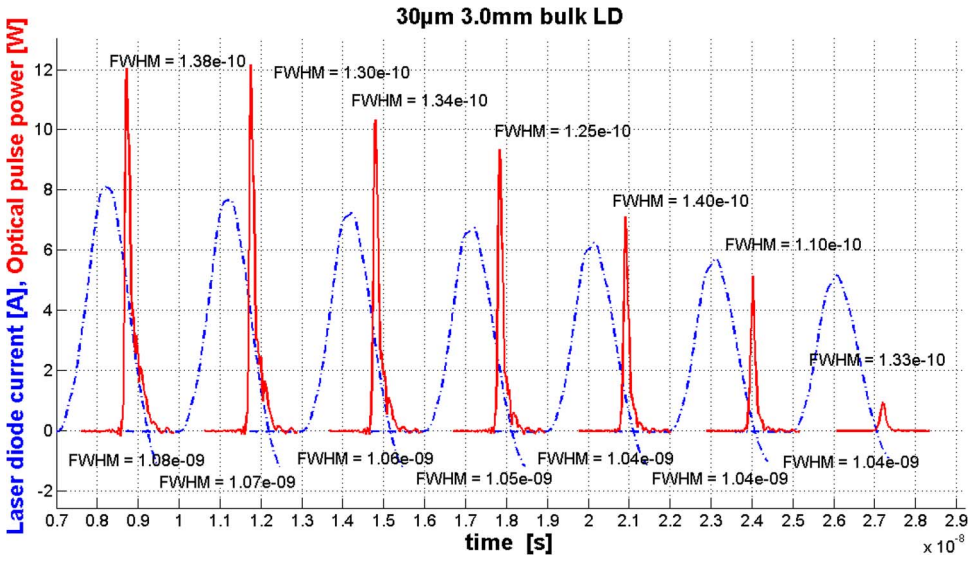

Fig. 2. Output (red curves) of a bulk laser diode with a cavity length of 3 mm and a stripe width of 30 μm at various driver current levels (blue curves).

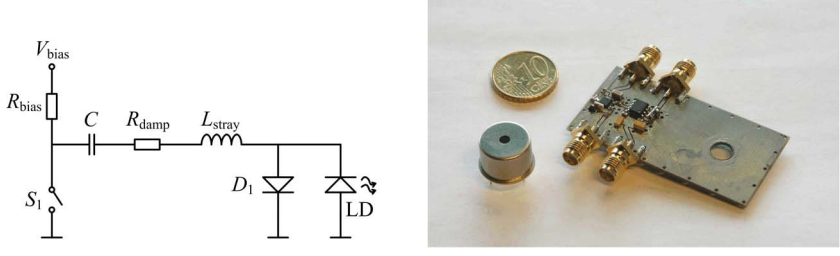

Fig. 3. MOS switch based driver scheme and transmitter board as used for the laser diode results given in Fig. 2.

necessity for high measurement speed. It should be noted that the laser is intended for operation at high currents to maximize the output pulse energy, which simultaneously minimizes the effect of temperature on the peak power. Our recent experiments show also that the temperature-induced deterioration of the laser performance can be reversed, at these high operating currents, by a relatively modest (about 20%) increase in the current pulse amplitude; more details will be presented elsewhere [37].

3. Performance Analysis

3.1. The Signal

In the following, we briefly analyze the performance of the pulsed TOF laser radar as described above with regard to the measurement range and measurement time. We start by looking into the rate of triggerings (signal) in the receiver channel as a function of the measurement range and system parameters and then discuss the effects of the background radiation (noise).

The strength of the received echo in a pulsed TOF radar follows the well-known laser radar equation given in (2) [31]. The form given here neglects the effects of non-overlapping axes (in the case of biaxial optics) and vignetting, since both these effects are present mainly at short distances [31]. It, however, predicts correctly the signal behavior at long distances, which

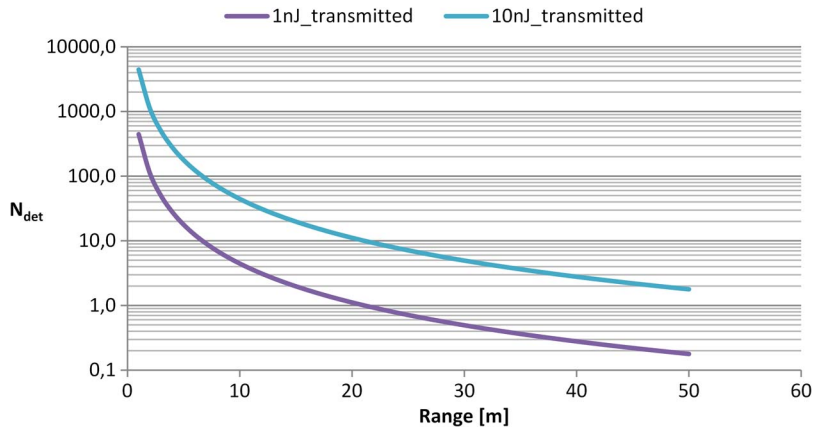

Fig. 4. Number of detected photons as a function of measurement range with 1 nJ and 10 nJ transmitted pulse energies: other parameters as in the text.

corresponds to the most important low SNR case. In (2), N_{ph} is the average number of photons seen by the receiver aperture (statistical variation follows the Poisson distribution), E_{tr} = transmitted pulse energy (1 nJ), ε_{opt} = efficiency of the optics (0.8), ρ_{target} = target reflectivity (0.08), A_{rec} = area of the receiver lens (2.5 cm^2), R = range (50 m), hc/λ_{tr} = photon energy (2.3×10^{-19} J). PDE (2% at 870 nm) is the photon detection efficiency of the SPAD and thus N_{det} can be considered as the average number of detected photons per single transmitted laser pulse. The parameters given in the parentheses correspond to the values used in the experiments as discussed in detail in Sections 4 and 5

$$N_{ph} = \frac{E_{tr} \times \varepsilon_{opt} \times \rho_{target} \times A_{rec}}{\pi \times R^2 \times h\frac{c}{\lambda_{tr}}}, \quad N_{det} = PDE \times N_{ph}. \tag{2}$$

As an example of typical values, Fig. 4 shows the number of detected photons per one laser pulse as a function of measurement range at the emitted energy levels of 1 nJ and 10 nJ. For example, with a pulse energy of 1 nJ and pulsing rate of 100 kHz, we can expect the receiver to trigger with a probability of 20% (thus the effective detection rate would be ~20 kHz) at the distance of 50 m to a non-cooperative target with a reflection coefficient of 8% (which is low). Since the diameter of the optics is only 18 mm, the result compares quite favorably with the linear detection techniques; see Section 6 and [38] for further details.

3.2. The Noise

Single photon detectors have two main noise sources, dark counts and the counts induced by background radiation. The level of the dark count rate depends on the area of the detector and is typically less than 10 kHz with a SPAD diameter of less than 20 μm in a 0.35 μm HV CMOS technology [29]. Thus the average time interval between the dark count induced triggerings is 100 μs. In reality, especially in outdoor applications, the random counts induced by the background radiation (the Sun) are much more frequent. The amount of background radiation falling onto a single SPAD detector follows roughly the equation

$$P_B \approx I_S \cdot A_{rec} \cdot \rho_{target} \cdot \left(\frac{FOV_{SPAD}}{2}\right)^2 \cdot BW_{opt} \tag{3}$$

where P_B = background power seen by the receiver [W], A_{rec} = area of the receiver lens [m^2], ρ_{target} = target reflectivity, FOV_{SPAD} = field of view of a single SPAD detector element roughly ϕ_{det}/f_{optics} in milliradians), and BW_{opt} = the optical bandwidth of the receiver [A] [32]. I_S is the

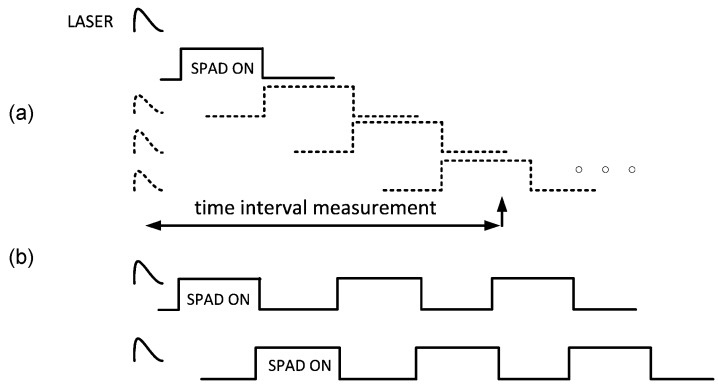

Fig. 5. Possible gating schemes for decreasing the probability of blocking of a SPAD receiver.

solar spectral irradiance $[\mathrm{W}/(\mathrm{m}^2\text{Å})]$. For example, an illumination level of 70 klux (bright sunlight) corresponds approximately to ~ 60 mW$/(\mathrm{str}\ \mathrm{m}^2\text{Å})$.

Using the equations above and knowing the system level parameters and detector properties, the average number of background triggerings introduced (or average mean time between triggerings) can be estimated quite easily. It is also seen that the optical bandwidth should obviously be limited as much as possible. However, due to drifts in the laser line and optical filter, a bandwidth of $\sim$40 nm is the smallest value practicable, unless a more expensive, stabilized laser design is used instead of a simple Fabry-Perot construction. Given the above values for the parameters and letting $\mathrm{FOV_{SPAD}} = 1$mrad (20 μm SPAD, $\mathrm{f_{focal,rec}} = 20$mm), we can estimate the mean time between photons hitting a single SPAD to be 1.7 ns $(\mathrm{P_B} = 120\ \mathrm{pW})$ and correspondingly between triggerings (PDP $= 2\%$), 85 ns at the 70 klux background illumination level $(\sim 60\ \mathrm{mW}/(\mathrm{str}^*\mathrm{m}^{2*}\text{Å}))$. This means that if the target is at a distance of 50 m, for example, which is equivalent to a time interval of 335 ns, the triggerings of the detector would be dominated by the background. Because of the Poisson characteristics of the background photons, the probability of background induced detection during the time interval ΔT follows the simple exponential law

$$p_{\mathrm{det}} = 1 - \exp\left(\frac{-\Delta T}{T_{\mathrm{mean}}}\right) \tag{4}$$

where $\mathrm{T_{mean}}$ is the mean time interval between the triggerings. Thus, with the above parameters, the probability of detection due to the random background photon would be $\sim$98% meaning that the receiver would be almost completely blocked out from the photons from the target. It is thus obvious that background radiation poses a serious challenge to a SPAD based laser distance measurement. This is emphasized by the fact that a SPAD once triggered needs a certain hold-off time ($\sim$10–20 ns in active quenching) before it can be biased again [25], [29]. Fortunately, however, it is known that a SPAD detector can quite easily be gated to be operative only for a certain period of time. By gating, the effective detection window of a SPAD can be shortened to ensure the level of background induced triggerings that the system can withstand. For example, Fig. 5 presents gating schemes, where a SPAD is repeatedly gated ON for a certain period of time, say 20 ns, for example, in successive measurements (a) or within the same laser shot and then quenched and held-off for another 20 ns before the next ON period (b). By reversing the sequence for the next pulse the whole range can be covered in just two laser shots. It is also possible to just let the SPAD work in free-running mode and minimize the quenching time to speed up the recovery. It is assumed, of course, that in the latter case as in case b, the system would include a multi-channel time-to-digital converter that can register and store all the hits within the laser shot before the actual hit from the target. If this is not available, the gating approach decreases the probability of getting a background hit during the ON time interval, and blocking is, thus, much less likely to occur.

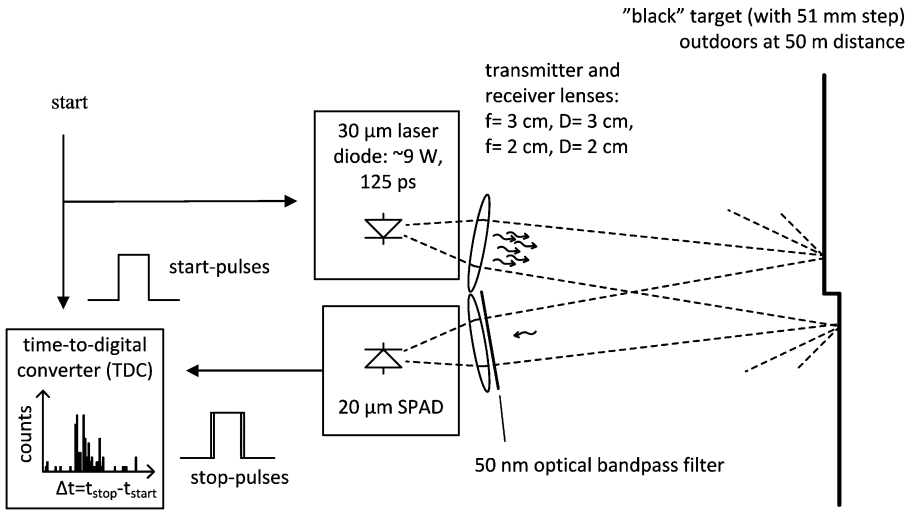

Fig. 6. Block diagram of the measurement configuration.

4. Measurement Configuration

The measurement configuration shown in Fig. 6 was constructed to validate the above analysis. The laser transmitter was using a bulk laser diode with a stripe width of 30 μm and energy of 1 nJ as explained above in Section 2.2. The detector was a single actively quenched CMOS SPAD with a diameter of 20 μm. The SPAD construction and electronics around the SPAD are described in more details in [33]. The control electronics of the SPAD detector were constructed in such a way that it was possible to gate the SPAD to be operative for a selected time period after laser triggering. To match the transmitter and receiver fields-of-view, the focal lengths of the transmitter and receiver optics were set to be 30 mm and 20 mm, respectively, giving a FOV of 1 mrad. The diameter of the effective aperture of the receiver optics was 18 mm giving an area of 2.5 cm^2. The receiver was equipped also with an optical interference filter having a bandwidth of 50 nm. The system included a time-to-digital converter capable of measuring the time interval between the emitted laser pulse and the received echo (digital output from the SPAD) with 25 ps single shot precision.

A photograph showing the construction of the optics, the transmitter, and the receiver together with the adjustments needed is shown in Fig. 7.

5. Measurement Results

In order to check the system performance, the following measurements were made: single-shot precision in single- and multi-photon detection mode, walk error, measurement range/measurement time, the effect of background radiation, and the possibility of its suppression by gating.

5.1. Single Shot Precision

The single-shot precision was measured to a non-cooperative target at a distance of 25 m. In the single photon detection mode, the received echo was attenuated with a neutral density filter so that only approximately 10% of the shots resulted in detection. In this mode, the distribution function of the results is the convolution of the laser pulse shape and time response of the SPAD. The corresponding result measured with a time interval resolution of 24.5 ps is given in Fig. 8(a). The FWHM value of the distribution is 150 ps as expected, since the pulse width the laser was measured to be 100 ps (see Fig. 2) and the expected jitter of the SPAD is around 50–100 ps. A slight asymmetry due to the diffusion tail of the SPAD and also due to the laser pulse shape is also seen. In addition, the precision was measured to a target that had a step of 5 cm

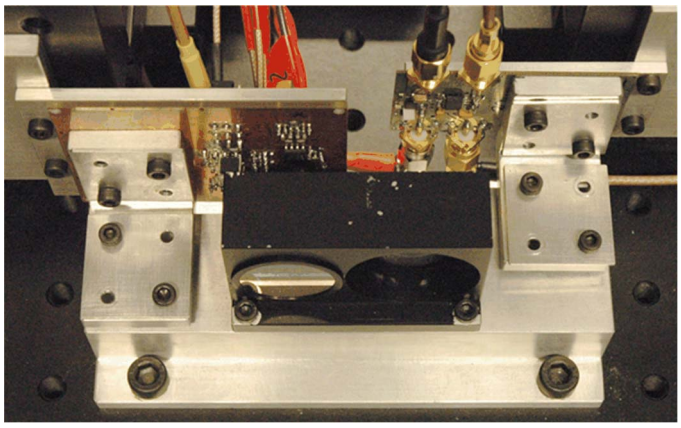

Fig. 7. SPAD laser radar laboratory set-up.

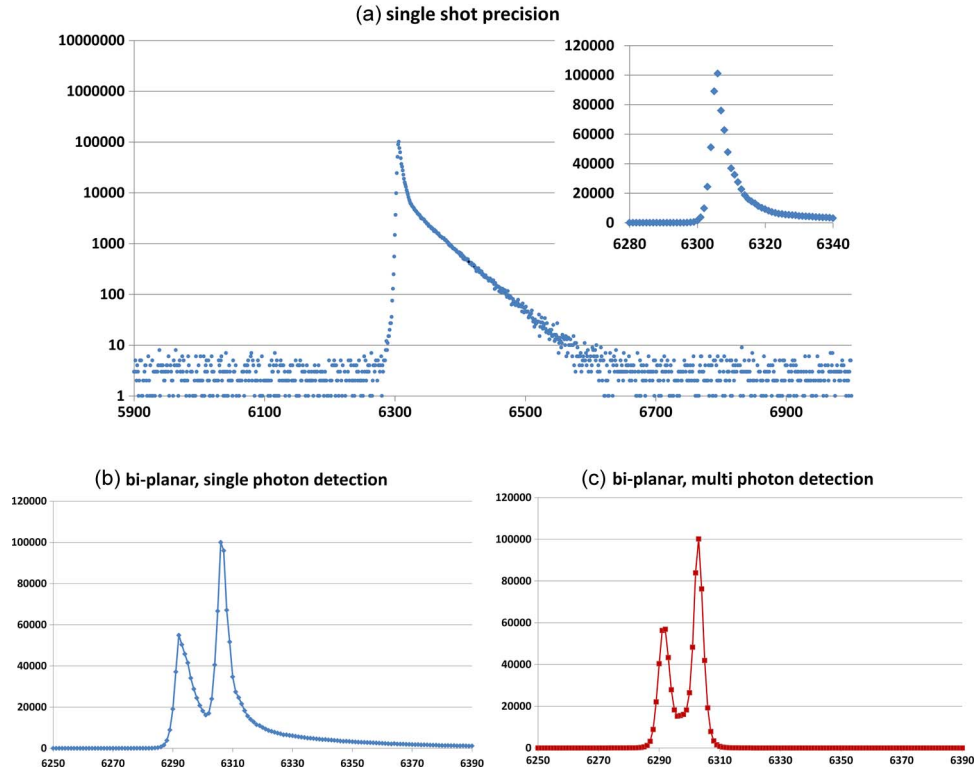

Fig. 8. Single shot distributions (x-axis: channel width = 24.5 ps, y-axis: number of hits). (a) Single photon detection mode, log scale (linear scale in the close-up). (b) Bi-plane target, single photon detection mode. (c) Bi-plane target, multi photon detection mode.

within the illuminated area. The results are shown in Fig. 8(b) in single photon detection mode and in Fig. 8(c) in the multi-photon detection mode (the latter being defined as the case when more than a single photon is assumed to initiate the avalanche breakdown). Note that in multi-photon detection mode, the apparent precision is improved since the detection probability now emphasizes the high power part of the laser pulse (around the peak), as opposed to the low power fronts.

It is also interesting to note that the single photon detection mode enables one to resolve the two target planes with a distance difference of 50 mm, which is, of course, not possible with a

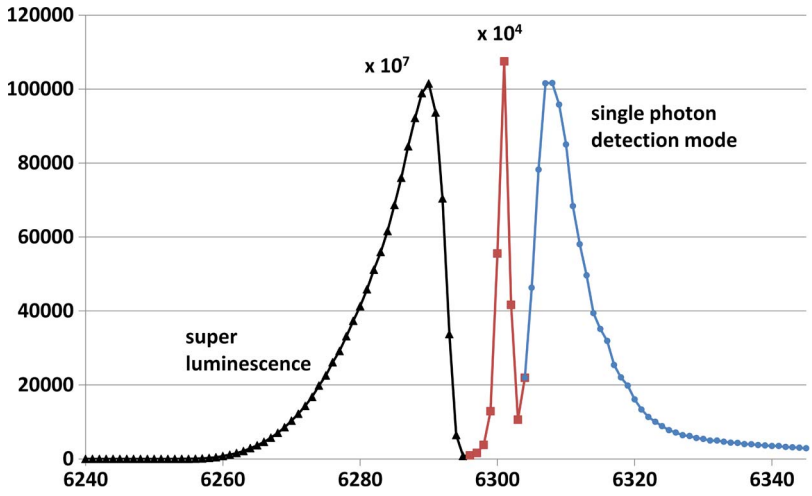

Fig. 9. Single shot distributions (y-axis: number of hits; x-axis: channel width = 24.5 ps) in a single photon detection mode (right, blue), 10 000 times higher received light intensity (in the middle, red), and ∼10 000 000 times higher received light intensity (left, black). Walk error defined as the distance of the leftmost and rightmost peak is ∼160 ps (equals to 24mm) within a dynamic range of $1 : 10^4$.

standard pulsed time-of-flight laser radar using longer pulses. Better precision can of course be achieved by averaging successive measurement results. It is well known that this improves the precision proportionally to the square root of the number of the measured results.

5.2. Walk Error

Walk error is arguably the most important systematic error source in a pulsed time-of-flight laser radar. It is produced by the varying energy of the received optical echo. The variation can be as large as 1 : 10 000 or even more since the reflection properties of the target may vary a lot. For example, in a traffic application a target which may once be a shining metal surface, may at some other time be covered by mud, and thus the intensity of the reflection may vary a lot. In pulsed time-of-flight laser radars utilizing pulses with a width of 3–5 ns, the walk error without compensation may range up to a few nanoseconds (geometrical error and the change in the effective electric delay of the receiver) [34].

In the true single photon detection mode there is no walk error since all detections are introduced by a single photon, and thus, the detection process is exactly identical no matter how often the detection happens. In reality, however, without any optical attenuator or transmitter energy control, the detection can be introduced by several photons. It is known that in this case the build-up of the avalanche multiplication is faster resulting in a walk error in simple threshold detection [35]. It should be noted, however, that in the multi-photon detection mode, also the detection probability is higher in the higher energy and/or earlier part of the pulse (depending on the strength of the reflection). These effects are clearly seen in the results shown in Fig. 9. Fig. 9 shows the single shot measurement distribution in single photon detection mode (rightmost curve, 8% non-cooperative target at the distance of ∼25 m) and another distribution measured from the target at the same distance but with 10 000× times higher received light power (middle curve). A walk error of ∼6.5channels or 160 ps is seen (calculated as the difference of the peak intensities). The result also clearly demonstrates the expected improvement of the precision in the multi-photon detection mode. The leftmost curve in Fig. 9 shows another distribution measured from the target at the same distance but with ∼10 000 000× times higher received light power (reflective tape). A larger walk error of 17.5 channels or 430 ps is noted. In this measurement the received echo is so strong that detections are received even before the steep rise of the laser pulse. This is not surprising since the laser diode emits spontaneous emission during the whole current pulse and, especially, the lasing evolves through super-luminescence at the

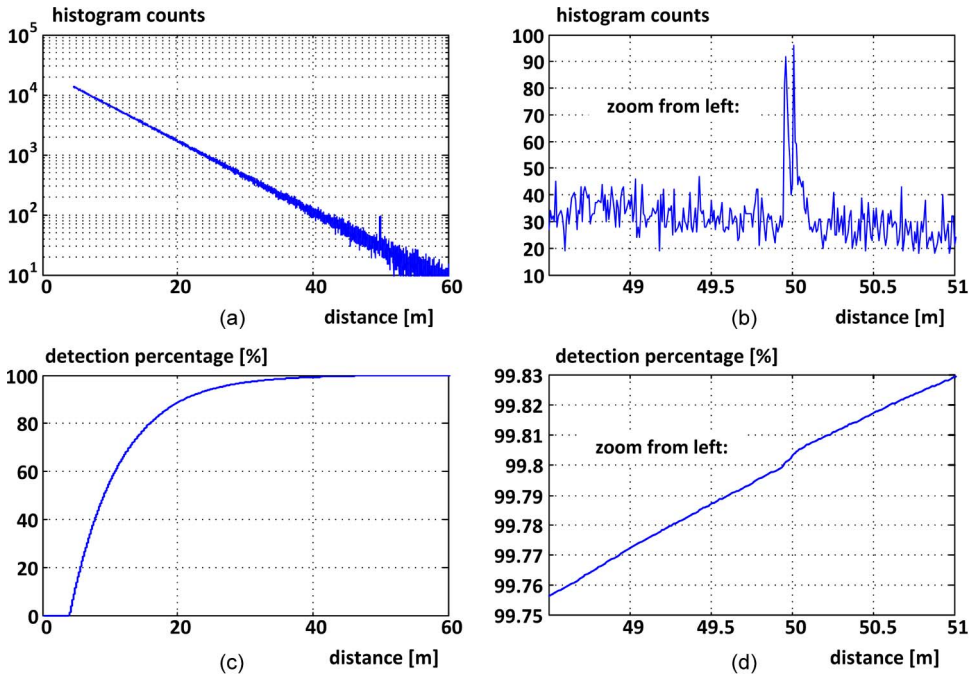

Fig. 10. (a) Distribution of measurement results from a target at 50 m in ∼100 klux background illumination and (b) a close-up from the range of signal detections. (c) Cumulative fraction of measurement results and (d) a corresponding close-up from the range of signal detections.

onset of the optical pulse. In fact, the effect of the super-luminescence is clearly seen in the leftmost curve of Fig. 9.

5.3. Measurement Range/Measurement Time

The measured detection probability from a diffuse target at the distance of 50 m and with a reflectance of 8% was 20% (1 detection for 5 laser shots), while the calculation with the parameters given above gives ∼17.5%. The only parameters which are not exactly known are the transmission of the optics (assumed to be 80%) and the PDP of the SPAD (assumed to be 2% at 870 nm). With these parameters, the agreement between the calculation and the measured rate is quite good

$$N_{\text{ph}} = \frac{1 \cdot 10^{-9} \cdot 0.8 \cdot 0.0785 \cdot 2.5 \cdot 10^{-4}}{\pi \cdot 50^2 \cdot 2.28 \cdot 10^{-19}} \approx 8.77$$

$$N_{\text{det}} = 0.02 \cdot 8.77 \approx 0.175 \quad \rightarrow \quad p_{\text{det}} \simeq 17.5\%$$

$$\text{measured} \rightarrow p_{\text{det}} \simeq 20\%.$$

The result indicates that assuming somewhat arbitrarily that 5 separate detections from the target are needed for a valid measurement result, an effective measurement rate of 10 kHz could be achieved to a target of 20% reflectance using a pulsing rate of 100 kHz.

The effect of background radiation was measured in bright sunshine with a non-cooperative target (8% reflectivity) at a distance of 50 m. The result of Fig. 10(a) shows the number of measured counts as a function of distance. As is seen in the figure, most of the counts (99.8%) were recorded as background hits before the target, which is shown as a small peak at the distance of 50 m. The distribution is exponential as expected and its time constant is about 45 ns (mean time between triggerings), which corresponds to 50-100 klux background illumination level. In this measurement the target is almost completely blocked out since only 0.01% of the measured results are from the target. Note, however, that as Fig. 10(b) shows, even in this

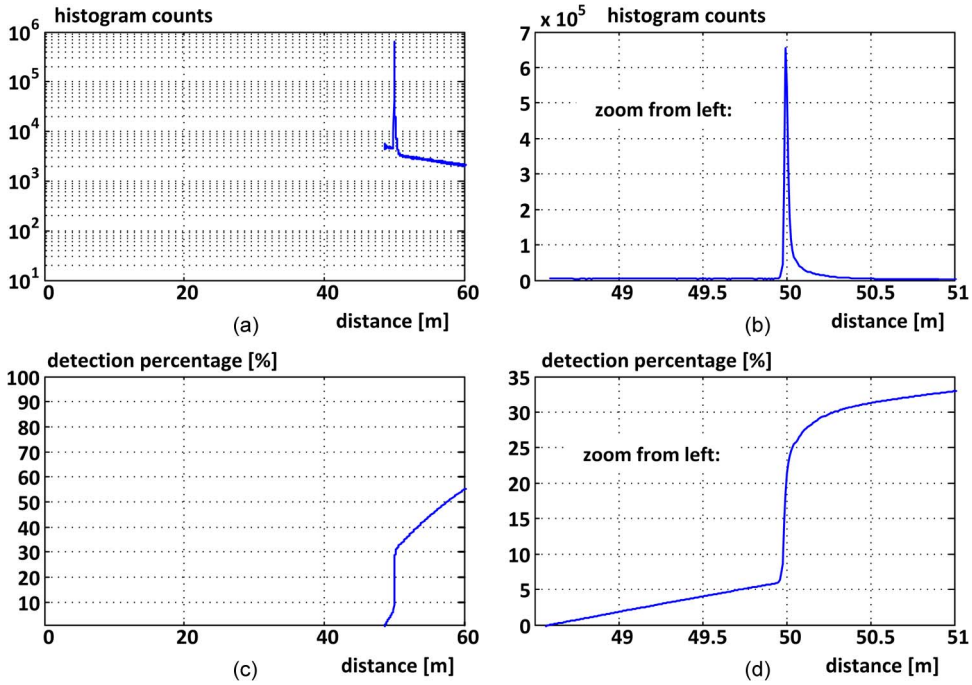

Fig. 11. (a) Distribution of measurement results from a target at 50m in ∼100 klux background illumination with a gate window of ∼10 ns and (b) a close-up from the range of signal detections. (c) A cumulative fraction of measurement results and (d) a corresponding close-up from the range of signal detections.

case, the bi-planar target can clearly be detected but only with a remarkably long measurement time.

Fig. 11 shows another result with a mono-planar target. In this measurement the SPAD was however switched on only ∼10 ns before the target. As a result, only 6% of the hits were recorded as background hits before the target. In this measurement, the background illumination level was slightly lower (mean time interval between BG triggerings ∼137 ns). As is also shown, about 20% of the results were recorded from the target. The reduction in the number of detected background hits follows closely the analysis given above.

6. Discussion and Summary

The above analysis and results show that the recently proposed new laser diode construction giving intensive (∼1 nJ) and short pulses (100 ps) from a relatively small emitting area ($\sim 2\ \mu\text{m} \times 30\ \mu\text{m}$) gives good promises for the transmitter of a pulsed time-of-flight laser radar working in single photon detection mode. The intensive pulses are advantageous since they increase the probability of target detection and, thus, improve the total ratio of target and background photons. It should be noted that an equal average energy with lower amplitude but higher rate pulses would give the same amount of target photons but unfortunately a higher background count as well. The high radiance of the transmitter is essential since it makes it possible to use a smaller field-of-view in the receiver and thus to strongly ($\propto \text{FOV}^2$) minimize the number of background photons. The effect of background illumination was also analyzed. It was shown that the gating of the SPAD detector is an effective means to avoid blocking of the receiver in case of high background illumination level. Instead of gating, another approach based on minimization of SPAD hold-off time and the use of multi-channel time interval measurement system can also be used.

The laser diode transmitter can be constructed with a small circuit area of 2–3 cm^2. The SPAD receiver and the time-to-digital converter can in principle be located on a single CMOS

die. Thus, the whole laser radar could have quite a compact construction. The results show that a single shot precision could be at the level of 2–3 cm. An effective measurement rate of >10 kHz is achievable to a non-cooperative target (20% reflectivity) at a distance of >50 m with an effective receiver aperture size of 2.5 cm^2 with the transmitted energy of 1 nJ. In the present system a single SPAD detector was used but the realization of the SPAD detector as a 2-D array would open up possibilities of relieving the mechanical tolerance of the optomechanics and its adjustments as well as to pave the way to 3-D imaging applications. The possibility for customized detector design makes is also relatively easy to include another detector array on the receiver die for the detection of the emitted laser pulse. Thus, a calibration channel can quite straightforwardly be realized, for example to minimize the temperature effects. Moreover, the gating approach could be used in co-axial optics to avoid the detector saturation effect caused by possible optical cross-talk.

Finally, it might be interesting to compare the proposed configuration to standard pulsed time-of-light laser radar employing linear detection techniques. As is shown above, with the given photon detection probability of 5% at 810 nm, the CMOS SPAD based detection would need approximately 20 photons for a valid detection. In linear detection case, the detection limit is determined by the noise of the receiver. Assuming that laser pulses with a length of 3 ns would be used, the receiver (avalanche photo diode, transimpedance preamplifier, post amplifiers, timing comparator) bandwidth would be around 200 MHz. For this kind of a receiver the typical level of input refereed noise current could be 5 $pA/\sqrt{Hz}$ [36] giving a total input noise of 70 nA_{rms}. Thus the minimum peak signal current needed for an SNR of 10 would be around 1 μA allowing some noise margin for the background noise. With the typical responsivity of the APD of around 30 A/W, the signal power needed would be around 30 nW. This means that approximately 400–500 photons (33 nW $\times$ 3 ns/2.3 $\times$ 10^{-19}) would be needed for a valid detection. With the optics and other parameters (18 mm receiver diameter, distance of 50 m, target reflectivity of 8%) specified above, this transforms to a laser peak power of 15 W (energy of 45 nJ), which can quite conveniently be generated with pulsed laser diodes.

In linear detection, the single shot precision is roughly proportional to the ratio of the rise time of received echo and signal to-noise ratio [36]. Thus with an SNR of 10 the precision is at the level of 150 ps which is just about the same as with the SPAD radar proposed above. The main systematic error of the measurement, the walk error, is caused in linear detection by two reasons. One of them is the pure geometrical effect due to varying amplitude and a constant threshold level. Thus this error is proportional to the rise time of the laser pulse. Another cause is the varying "effective delay" of the receiver channel, which for a small signal is proportional to its effective RC constant ($\sim$1 ns for 200 MHz bandwidth)and for large signal is much smaller [34], [36]. In total, the walk error in linear detection is 2–3 ns typically and thus markedly larger than what was measured above with the SPAD radar ($\sim$160 ps within a range of 1 : 10 000). It should be noted also that for the SPAD radar in pure single photon detection mode, the walk error is totally absent.

Thus, from the point of view of performance the laser radar configurations compared above are not radically different. The main advantage of the SPAD based approach is its simplicity which arises from the fact that no separate avalanche photo detector and its high-voltage bias source nor the quite sophisticated linear amplifier channel (and its high current consumption) are needed. On the other hand, the tolerance of the receiver based on linear detection to background illumination is higher. In linear detection the background illumination produces shot noise that adds up with electronic noise of the receiver. For example, assuming a background noise level of 10 nW (higher than above since the FOV of the receiver is also typically higher), the shot noise produced at the receiver input with the typical APD parameters (excess noise factor of 3, gain 60) would be around 60 nArms, thus being approximately at the same level as the electronic noise of the receiver.

It is obvious that the main concern with the SPAD based pulsed time-of-light laser radar is the rather low photon detection probability of a silicon (Si) based CMOS SPAD at wavelengths longer than 800 nm, which in this work has been partly compensated for with a high-energy and

yet high speed laser diode transmitter. In 1-D measurements especially, a SPAD detector based on III-V compound semiconductors would be an interesting option, but in near-range 2-D and 3-D measurements the high system integration level achievable with the Si-based SPAD or SPAD array is attractive.

References

[1] S. Donati, *Electro-Optical Instrumentation: Sensing and Measuring With Lasers*. Upper Saddle River, NJ, USA: Prentice-Hall, 2004.
[2] M. Xuesong, D. Inoue, S. Kato, and M. Kagami, "Amplitude-modulated laser radar for range and speed measurement in car applications," *IEEE Trans. Intell. Transp. Syst.*, vol. 13, no. 1, pp. 408–413, Mar. 2012.
[3] D. C. Carmer and L. M. Peterson, "Laser radar in robotics," *Proc. IEEE*, vol. 84, no. 2, pp. 299–320, Feb. 1996.
[4] B. Schwarz, "LIDAR: Mapping the world in 3D," *Nature Photon.*, vol. 4, pp. 429–430, 2010.
[5] K. Fuerstenberg and F. Ahlers, "Development of a Low Cost Laser Scanner—The EC Project MiniFaros," in *Advanced Microsystems for Automotive Applications 2011, Smart Systems for Electric, Safe and Networked Mobility*, G. Meyer, J. Valldorf, Eds. Berlin, Germany: Springer-Verlag, 2011.
[6] V. C. Coffey, "Imaging in 3-D: Killer apps coming soon to a device near you!" *Opt. Photon. News*, vol. 25, no. 6, pp. 36–43, 2014.
[7] R. McIntyre, "Comparison of photomultipliers and avalanche photodiodes for laser applications," *IEEE Trans. Electron Devices*, vol. ED-17, no. 70, pp. 347–352, Apr. 1970.
[8] S. N. Vainshtein, V. S. Yuferev, and J. T. Kostamovaara, "Avalanche transistor operation at extreme currents: Physical reasons for low residual voltages," *Solid-State Electron.*, vol. 47, no. 8, pp. 1255–1263, Aug. 2003.
[9] S. Vainshtein, J. Kostamovaara, A. Kilpela, and K. Maatta, "A high-speed, high current driver for operation with low ohmic load," *Electron. Lett.*, vol. 33, no. 10, pp. 904–906, May 1997.
[10] K. Ito *et al.*, "System design and performance characterization of a MEMS-based laser scanning time-of-flight sensor based on a 256 $\times$ 64-pixel single-photon imager," *IEEE Photon. J.*, vol. 5, no. 2, pp. 559–572, Apr. 2013.
[11] C. Niclass, C. Favi, T. Kluter, F. Monnier, and E. Charbon, "Single-photon synchronous detection," *IEEE J. Solid-State Circuits*, vol. 44 , no. 7, pp. 1977–1989, Jul. 2009.
[12] R. J. Walker, J. A. Richardson, and R. K. Henderson, "A 128 $\times$ 96 pixel event-driven phase-domain $\Delta\Sigma$-based fully digital 3D camera in 0.13 μm CMOS imaging technology," in *Proc. IEEE ISSCC*, 2011, pp. 410–412.
[13] F. Villa *et al.*, "CMOS imager with 1024 SPADs and TDCs for single-photon timing and 3-D time-of-flight," *IEEE J. Sel. Topics Quantum Electron.*, vol. 20, no. 6, Nov./Dec. 2014, Art. ID. 3804810.
[14] C. Niclass *et al.*, "Design and characterization of a 256 $\times$ 64-pixel single-photon imager in CMOS for a MEMS-based laser scanning time-of-flight sensor," *Opt. Exp.*, vol. 20, no. 11, pp. 11 863–11 881, May 2012.
[15] C. Niclass, C. A. Rochas, P.-A. Besse, and E. Charbon, "Design and characterization of a CMOS 3-D image sensor based on single photon avalanche diodes," *IEEE J. Solid-State Circuits*, vol. 40, no. 9, pp. 1847–1854, Sep. 2005.
[16] C. Niclass, M. Soga, H. Matsubara, M. Ogawa, and M. Kagami, "A 0.18 μm CMOS SoC for a 100-m-range 10-frame/s 200 $\times$ 96-pixel time-of-flight depth sensor," *IEEE J. Solid-State Circuits*, vol. 49, no. 1, pp. 315–330, Jan. 2014.
[17] D. Bimberg, K. Ketterer, E. H. Bottcher, and E. Scoll, "Gain modulation of unbiased semiconductor lasers: Ultrashort pulse generation," *Int. J. Electron.*, vol. 60, no. 23, pp. 23–45, 1986.
[18] B. Ryvkin, E. Avrutin, and J. Kostamovaara, "Asymmetric-waveguide laser diode for high-power optical pulse generation by gain switching," *IEEE/OSA J. Lightw. Technol.*, vol. 27, no. 12, pp. 2125–2131, Jun. 2009.
[19] B. Ryvkin, E. A. Avrutin, and J. T. Kostamovaara, "Quantum Well laser with an extremely large active layer width to optical confinement factor ratio for high-energy single picosecond pulse generation by gain switching," *Semicond. Sci. Technol.*, vol. 26, no. 4, Apr. 2011, Art. ID. 045010.
[20] L. W. Hallman *et al.*, "Asymmetric waveguide laser diode operated in gain switching mode demonstrates high power optical pulse generation," *Electron. Lett.*, vol. 46, no.1, pp. 65–66, Jan. 2010.
[21] B. S. Ryvkin, E. A. Avrutin, and J. T. Kostamovaara, "Vertical cavity surface emitting lasers with the active layer position detuned from standing wave antinode for picosecond pulse generation by gain switching," *J. Appl. Phys.*, vol. 110, no. 12, Dec. 2011, Art. ID. 123101.
[22] B. Lanz, B. Ryvkin, E. Avrutin, and J. Kostamovaara, "Performance improvement by a saturable absorber in gain-switched asymmetric-waveguide laser diodes," *Opt. Exp.*, vol. 21, no. 24, pp. 29 780–29 791, Dec. 2013.
[23] S. Riecke *et al.*, "23 W peak power picoseconds pulses from a single-stage all-semiconductor master oscillator power amplifier," *Appl. Phys. B*, vol. 98, no. 2/3, pp. 295–299, Feb. 2010.
[24] S. Riecke *et al.*, "10.7W peak power picoseconds pulses from high-brightness photonic band crystal laser diode," *Electron. Lett.*, vol. 46, no. 20, pp.1393–1394, Sep. 2010.
[25] A. Rochas *et al.*, "Low-noise silicon avalanche photodiodes fabricated in conventional CMOS technologies," *IEEE Trans. Electron Devices*, vol. 49, no. 3, pp. 387–394, Mar. 2002.
[26] J. Jansson, V. Koskinen, A. Mäntyniemi, and J. Kostamovaara, "A multi-channel high precision CMOS time-to-digital converter for laser scanner based perception systems," *IEEE Trans. Instrum. Meas.*, vol. 81, no. 9, pp. 2581–2590, Sep. 2012.
[27] D. Tamborini, B. Markovic, F. Villa, and A. Tosi, "16-channel module based on a monolithic array of single-photon detectors and 10-ps time-to-digital converters," *IEEE J. Sel. Topics Quantum Electron.*, vol. 20, no. 6, pp. 1–8, Nov./Dec. 2014.
[28] B. S. Ryvkin, E. A. Avrutin, B. Lanz, and J. T. Kostamovaara, "Strongly asymmetric waveguide semiconductor lasers for picosecond pulse generation by gain- and Q-switching," in *Proc. 16th Int. Conf. Transparent Opt. Netw.*, Graz, Austria, Jul. 6–10, 2014, pp. 1–4.

[29] L. Pancheri and D. Stoppa, "Low-noise CMOS single-photon avalanche diodes with 32 ns dead time," in *Proc. 37th ESSDERC*, 2007, pp. 362–365.
[30] L. W. Hallman, J. Huikari, and J. Kostamovaara, "A high-speed laser transmitter for single photon imaging applications," in *Proc. IEEE SENSORS Conf.*, 2014.
[31] J. Wang and J. Kostamovaara, "Radiometric Analysis and Simulation of Signal Power Function in a Short-Range Laser Radar," *Applied Optics*, vol. 33, no.18, pp. 4069–4076, 1994.
[32] J. L. Button, "Laser altimetry measurements from aircraft and spacecraft," *Proc. IEEE*, vol. 77, no. 3, pp. 463–477, Mar. 1989.
[33] I. Nissinen *et al.*, "A sub-ns time-gated CMOS single-photon avalanche diode detector for Raman spectroscopy," in *Proc. ESSDERC/ESSCIRC*, 2011, pp. 375–378.
[34] P. Palojärvi, T. Ruotsalainen, and J. Kostamovaara, "A 250-MHz BiCMOS receiver channel with leading edge timing discriminator for a pulsed time-of-flight laser rangefinder," *IEEE J. Solid-State Circuits*, vol. 40, no. 6, pp. 1341–1349, Jun. 2005.
[35] E. Samain, "Timing of optical pulses by a photodiode in the Geiger mode," *Appl. Opt.*, vol. 37, no. 3, pp. 502–506, Jan. 1998.
[36] S. Kurtti and J. Kostamovaara, "An integrated laser radar receiver channel utilizing a time-domain walk error compensation scheme," *IEEE Trans. Instrum. Meas.*, vol. 60, no. 1, pp. 146–157, Jan. 2011.
[37] J. M. T. Huikari *et al.*, "High-energy picosecond pulse generation by gain switching in asymmetric waveguide structure multiple quantum well lasers," *IEEE J. Sel. Topics Quantum Electron.*, submitted for publication.
[38] T. Ruotsalainen, P. Palojärvi, and J. Kostamovaara, "A wide dynamic range receiver channel for a pulsed time-of-flight laser radar," *IEEE J. Solid-State Circuits*, vol. 36, no. 8, pp. 1228–1238, Aug. 2001